

Journal of Stress Analysis

Vol. 8, No. 2, 2023-24, 51-63



ORIGINAL RESEARCH PAPER

Modeling and Investigation of Semi-Elliptical Cracks in the Weld Seam of Pressurized Cylindrical Tanks

Hadi Eskandari*⁰, Arash Bahrami

Abadan Institute of Technology, Petroleum University of Technology, Abadan, Iran.

Article info

Article history: Received 15 January 2024 Received in revised form 22 February 2024 Accepted 08 March 2024

Keywords:
Stress intensity factor
Semi-elliptical crack
Cylindrical pressure vessel
Weld seam
ANSYS

Abstract

This work examines the finite element model of three-dimensional semielliptical fractures in a cylindrical pressure tank. The three-dimensional semi-elliptical cracks in cylindrical pressure tubes are investigated using the ANSYS finite element analysis software. The primary goals of this study are as follows. First, codes for the ANSYS parametric design language (APDL) were created to make it easier to simulate various semi-elliptical fracture topologies in cylindrical pressure vessels. The second is to use these codes to investigate the impact of certain problem factors on the normalized stress intensity coefficient distribution for cracks. Some of these properties include the crack depth ratio (DDR) and crack aspect ratio (ACR). Furthermore, a semi-elliptical fracture in the tank body connection at the weld seam is considered to investigate the effect of shape transfer on the normalized stress intensity coefficient distribution. By reducing the thickness, we see the increase and improvement of the stress intensity factor. Also, cracks with ac = 0.04 are a dangerous type and have a faster growth and progression rate than other types of ac = 0.6, 0.8 and 1. Cracks with ac = 1 have the lowest stress intensity factor. In the case of at = 0.8, which has the lowest possible thickness, the stress intensity factor is the highest. The highest stress intensity coefficient is at the crack tip. With the increase of ac, a decrease in the stress intensity factor is seen, in which case the cracks with at = 0.8 and the lowest thickness have a higher stress intensity factor, which is at the top of the crack. ac = 1.2 has the lowest stress intensity factor. As seen, the higher the aspect ratio, the smaller the values of stress intensity factors. In other words, the higher the relative crack depths, the higher the stress intensity factor.

Nomenclature

K_0	Normalizing stress intensity factor	LBB	Leak-Before Break
K_{I}	Mode I stress intensity factor	LEFM	Linear-Elastic Fracture Mechanics
K_{II}	Mode II stress intensity factor	SIF	Stress Intensity Factor
K_{III}	Mode III stress intensity factor	$\mid E \mid$	the modulus of elasticity
P	Internal pressure	Q	Flaw shape factor
$\sigma\theta\theta$	Hoop stress component	α	Depth of semi-elliptical surface crack
\emptyset , θ	Parametric angle of crack	APDL	ANSYS Parametric Design Language

^{*}Corresponding author: H. Eskandari (Associate Professor)

E-mail address: hadi.nioc@gmail.com doi 10.22084/JRSTAN.2025.29380.1258





FEA	Finite Element Analysis	HAZ	HEAT AFFECTED ZONE
PWHT	Post weld heat treatment	ϑ	Poisson's ratio
R_i	Inner radius of the spherical pressure ves-	R_0	Outer radius of the spherical pressure
	sel		vessel
c	Half-length of semi-elliptical surface	t	Wall thickness of the spherical pressure
	crack		vessel
FEM	Finite Element Method		

1. Introduction

A pressure vessel is a closed container that holds gases or liquids at pressures significantly more significant than the ambient air. The history of pressure vessel construction and operation has shown that the pressure difference is hazardous and has resulted in deadly accidents [1].

Nowadays, businesses utilize several spherical and cylindrical pressure vessels to carry gases and liquids under pressure. The primary reasons for cylindrical pressure vessels' success in various industries are their perfect specific strength (strength/weight) and ease of packaging. Furthermore, cylindrical pressure vessels are the only alternative at any site where extremely high pressures are utilized, including explosion containment tanks or storing certain oil and gas materials in the oil and gas industry, because the tanks are highly prone to breaking. Severe corrosion occurs under pressure loading circumstances.

Many different sectors and businesses employ cylindrical pressure vessels, including chemical and process industries, thermal and nuclear power plants, fluid delivery systems, and space exploration [2].

Numerous failures of pressure vessels have been connected to surface fissures. Reliable evaluations of fracture strengths and crack-growth rates of these surface-cracked components require precise stress measurements. Because of the complexity of these problems, all researches have used approximative analytical methods or engineering estimations to determine stress-intensity variables.

One of the most prevalent kinds of cracks in pressure vessels is the semi-elliptical crack. These fissures are elliptical in shape, with one side being flat and the other side being curved. Pressure vessel failure and stress concentration can be greatly impacted by the presence of semi-elliptical cracks. Thus, it is imperative to look into how semi-elliptical cracks affect pressure vessel failure [14].

Barata [3] used the load relief factor, an approximation, to calculate the stress intensity factor (SIF) of several fractures on the inner surface of a thick-walled vessel subjected to internal pressure. The validity of this method was determined by first determining the SIF for current standard problems and then comparing the same derivatives using this method. The obtained difference was determined to be 20%, which seems con-

servative. As a result, the SIFs of many edge fractures on the inner surface of the vessel that were located symmetrically (along the radial direction) were calculated.

A study by Liu et al. examined the impact of cracks on the fracture behavior of a pressure vessel made of aluminum alloy and found that the presence of cracks significantly affects the vessel's fracture behavior and that larger crack sizes increase the likelihood of failure. Another study by Lee et al. examined the impact of cracks on the fatigue crack growth behavior of a pressure vessel made of high-strength low-alloy steel and found that the presence of cracks significantly affects the crack growth rate and, consequently, the fatigue life of the vessel [14, 15].

When a component cracks, it can no longer do the function for which it was designed. When it comes to pressure vessels, this could cause a rupture that might endanger the surrounding personnel or other buildings. Because of the responsibilities that the components have in the assembly, fractures will cause damage to differing degrees. The entire structure depends on one part, therefore in the worst case, if it fails, it will collapse.

The fracture analysis method known as linearelastic fracture mechanics (LEFM) implies that a specimen has a fault or crack, that the crack is a flat surface inside a linear elastic stress field, and that the energy released during the rapid propagation of the crack is a fundamental attribute of the material independent of the component size [4].

Numerous investigations have been carried out to examine the behavior of pressure vessels with semi-elliptical surface cracks. Kim and Park's study examined the impact of crack depth on the crack propagation behavior in a pressure vessel and discovered that as crack depth increased, the crack propagation rate increased and the vessel's remaining life decreased [13].

The stress intensity variables can provide details about the stress field around the fracture point. They are defined by the magnitude of the singular stress and displacement fields, i.e., the local stresses and displacements surrounding the fracture tip. The specimen's geometric limits, loading, crack size, and form all affect the SIF. Failure will occur when the fracture toughness, also known as SIF, gets closer to its critical value [5].

SIF is calculated for each of the three types of crack

tip displacement (I, II, or III), taking into account the crack's shape and length, as well as the effects of applied loads. Therefore, the size of the fracture tip stress field for a particular mode of propagation equals the stress intensity factor for a homogeneous linear elastic material [5].

The crack propagation rate rises as the crack size and depth grow, according to analytical and numerical data. Additionally, we see that when crack size and depth increase, the vessel's remaining life reduces. Additionally, we discover that the crack orientation has a substantial impact on the crack propagation behavior, with the maximum propagation rate occurring in cracks orientated parallel to the loading direction [11].

Here, displacement values of the nodes at the crack front are used to determine SIF after modeling and problem-solving with the use of finite element method (FEM).

Raju and Newman [6] used three-dimensional finite element modeling to examine longitudinal fractures in pressurized cylinders. They limited their analysis to Mode I. Their findings indicated that depending on the loading and geometry, the fracture's most profound or corner sites have the highest stress intensity factor. Furthermore, the stress intensity factor for external cracks is higher than for interior ones.

Lin and Smith [7] examined a few geometry and crack possibilities. Through the use of three-dimensional finite element modeling, their results show that fatigue fractures evolve in a semi-elliptical shape independent of the initial shape of the crack; in other words, they demonstrated that cracks of any shape will ultimately take on a semi-elliptical shape.

Lin and Smith [8] demonstrated that semi-elliptical cracks, whose centers lie on bar surfaces, or semicircular fractures, whose centers move along cylinder radii, are suitable models for simulating real-world cracks. In real industrial applications, cracks frequently occur in the weld seam zone where pressure vessels are connected to input/output flanges

The FEM took into account the crack behavior in the weld seam for the first time because of the numerous failures brought on by the expansion of cracks in the weld seam.

In this study, the software was used to model the pressure tank and the weld seam crack once the problem was defined. The appropriate boundary conditions were then added on the model after it was meshed. Lastly, the graphs and output data from the validation software were analyzed.

Therefore, it is crucial to take into account the presence of cracks in the design and operation of pressure vessels to ensure their safe and dependable operation. Overall, the literature indicates that cracks are a critical factor in predicting the failure of pressure vessels. Experimental studies and numerical simulations have demonstrated that cracks significantly affect the frac-

ture behavior and fatigue life of pressure vessels.

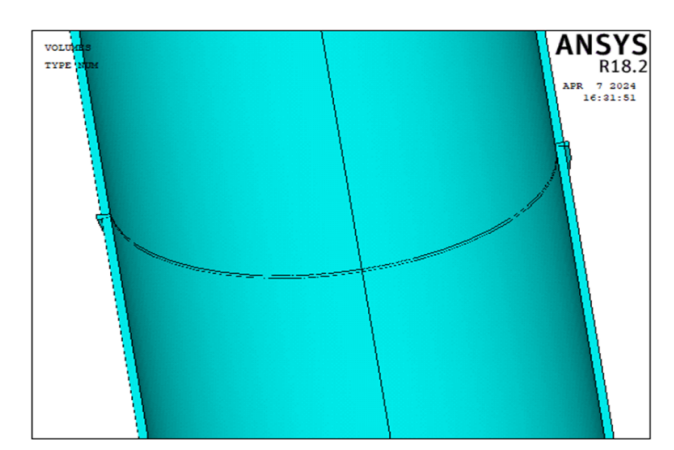
2. Materials and Method

This paper analyzes two semi-elliptic crack instances. Since adjusting a/c and a/t can yield acceptable approximations to actual fracture forms, semi-elliptic shapes are commonly employed in the literature.

The 3D analysis is performed on an elastic cylindrical pressure vessel with an inner radius (Ri), outer radius (Ro), and wall thickness of (t) (Fig. 1), where the wall thickness is constant. The model consisted of a cylindrical pressure vessel containing a semi-elliptical surface crack inside the weld seam, with crack length c and depth a, as seen in Fig. 2.

This study covers a wide range of vessel geometries and crack configurations a/c=0.2,0.4,0.6,0.8,1 and 1.2 and a/t=0.2,0.4,0.6,0.8.

The 3D analysis is performed on a cylinder with inner radius Ri, outer radius Ro and constant wall thickness t (Fig. 3). Fig. 4 shows a semi-elliptical surface crack inside a weld seam in a cylindrical pressure vessel at the body junction with half the length (c) and depth (a). The stress intensity factor was somewhat influenced by adjusting the length of the cylindrical segment.



 ${\bf Fig.~1.}$ Schematic representation of the problem.

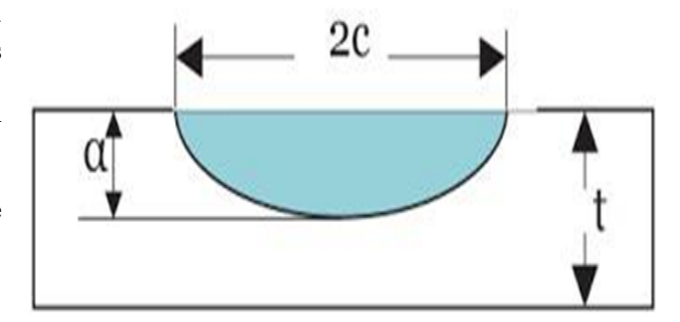


Fig. 2. Crack configuration.

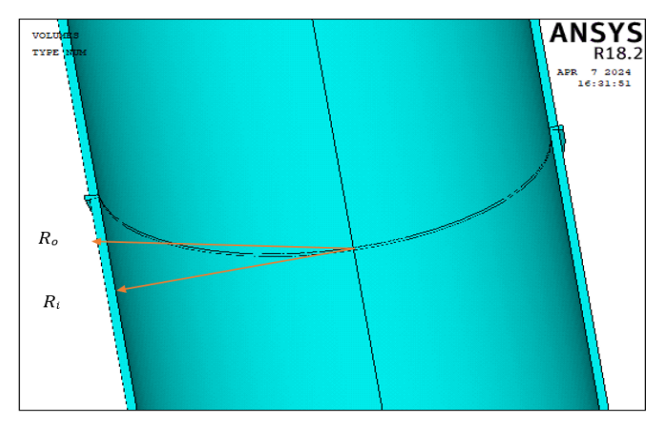


Fig. 3. Crack configuration located at the connection between the cylinder and the welding seam.

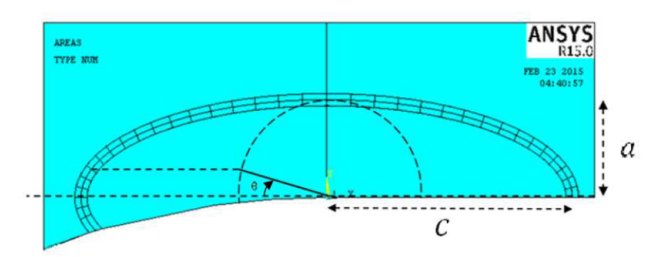


Fig. 4. Defining the parameters of the crack located at the junction of the cylinder and the weld.

Many engineering constructions have welded connections that crack often. The evaluation of fatigue and fracture is greatly aided by practical examinations of such cracks.

Due to the complex geometry of the joints, a high stress gradient occurs at the weld toe, creating a localized notch effect. The SIF value is raised by this impact [9].

Semi-elliptical surface cracks located at the weld toe of welded joints often propagate and lead to the failure of structural components. As such, evaluating the structural integrity of broken welded connections is practically crucial. The SIF (K), which controls the intensity of the stress field at the crack tip, is commonly used for assessing the fatigue and fracture resistance of such faulty structures [10].

As shown in Fig. 5(1), the crack front region was produced by swiping an auxiliary area around the crack front line. After that, the produced volume known as a "crack tunnel" is created using non-singular finite elements in the remaining length of the crack tunnel and singular finite elements surrounding the fracture front (Fig. 5(2)). Following this, half of the model was created by meshing and sweeping the cylinder's cross-section on the fractured plane in two phases (Fig. 5.3-4).

Quadratic displacement behavior is seen by the 20node solid element SOLID186 in three dimensions. The element is composed of 20 nodes, each of which has three degrees of freedom: translations in the nodal x, y, and z dimensions. Plasticity, hyper elasticity, creep, stress stiffening, large deflection, and large strain capabilities are all supported by the element. Additionally, it can simulate the deformations of completely incompressible hyperplastic materials and virtually incompressible elastoplastic materials using mixed formulation capabilities.

SIF has a unique use in researching failure mechanics and crack development issues. In order to quantify singularity, Irwin developed the idea of SIF. He demonstrated that the distribution of all the elastic forces surrounding the crack point was the same.

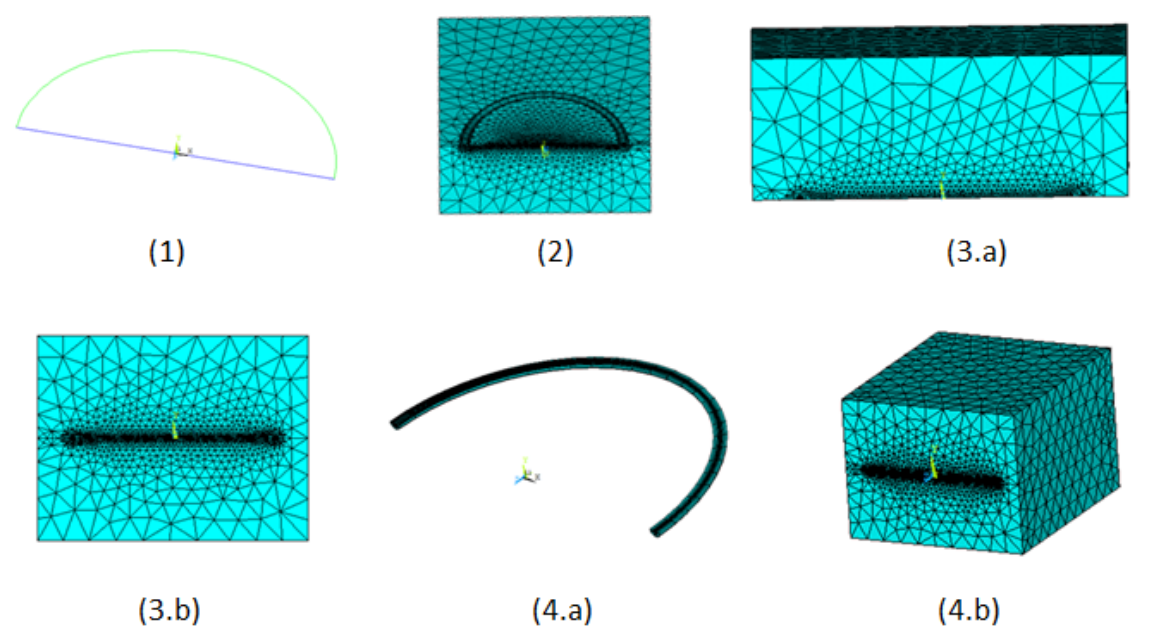


Fig. 5. Finite element model: 1) crack front generation, 2) Half crack model 3a) Mesh generation of the crack plane, 3b) The complete crack box in front 4a) Crack tunnel 4b) Another complete crack view box.

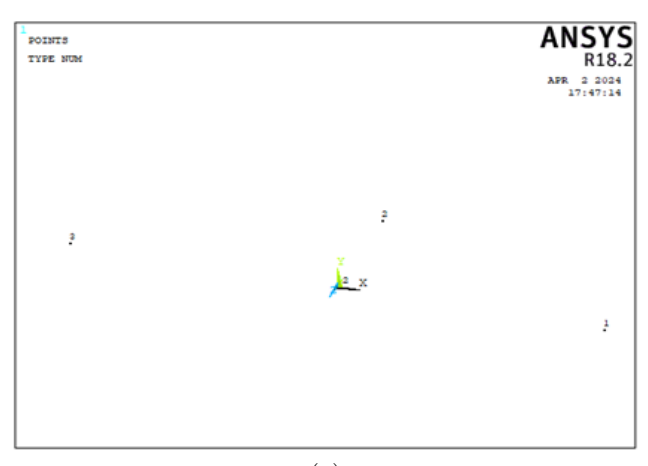
Consequently, the expression regulates the amount of local stress. The locations of external boundaries determine the $K_{\rm I}$, $K_{\rm II}$, and $K_{\rm III}$ factors according to the definition used to compute the stresses surrounding the fracture tip. The SIF, which is given as MPa \sqrt{m} in fracture mechanics, showed the extent of stress concentration at the tip of a longitudinal crack [12].

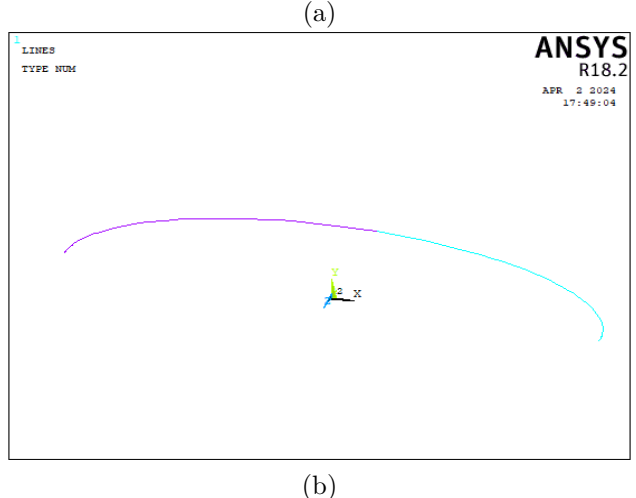
$$K_{I,\ II,\ III} = \sigma_A \sqrt{\pi a} = \sigma_{ij} \sqrt{2\pi ri}$$

Where σ_A is the applied stress and a is the crack length.

3. Modeling

To model semi-elliptical cracks in cylindrical pressure vessel, some keypoints are created initially to form the crack front line (Fig. 6a). Keypoint No. 1 is included in a semicircular region made perpendicular to the plane on which key points are made. In the subsequent processes, this region is formed to form the tubular volume surrounding the fracture front. Next, an elliptical path is formed by drawing lines connecting these key points, as seen in Fig. 6b. The area generated at Keypoint 1 is dragged along the lines to produce a tubular volume around the fracture front (Fig. 6c).





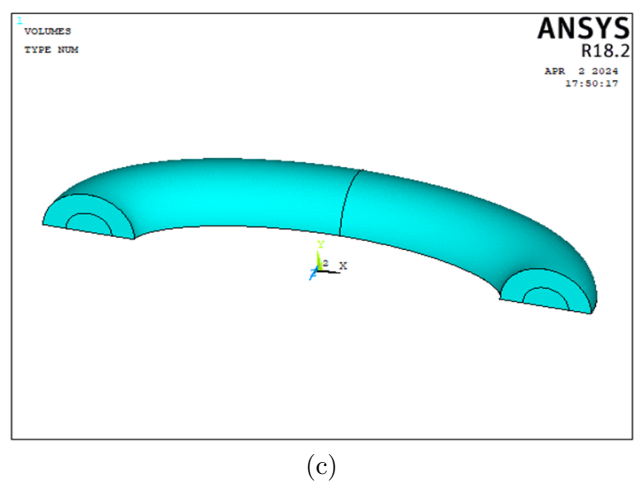


Fig. 6. a) Keypoints on the crack front. b) Lines on the crack front. c) Volumes created on the crack front.

After the creation of volumes around the crack tunnel and modeling the parts needed to complete the cylindrical vessel, the model is ready for meshing and analysis. (Figs. 7 and 8).

Pressure vessel and weld metal data are given in Tables 1, 2, and 3.

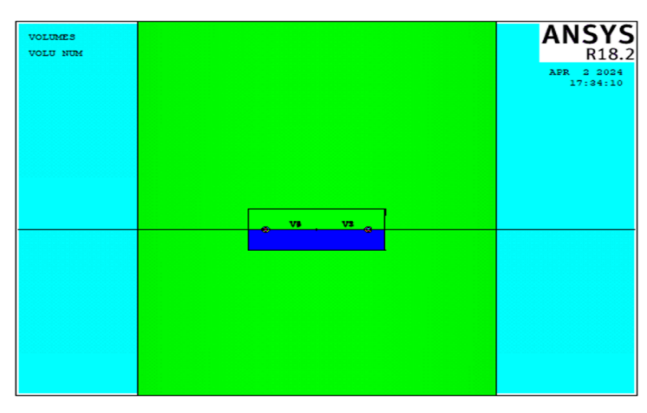


Fig. 7. Semi-elliptical crack in cylindrical vessel (half of model).

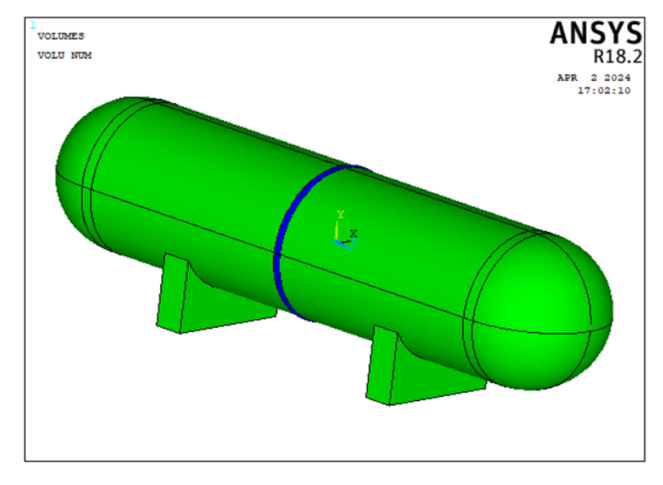


Fig. 8. Profile of the vessel and welding line.

 $\begin{array}{l} \textbf{Table 1} \\ \textbf{Pressure vessel design data}. \end{array}$

	Technic	al data		
Calculation and design		ASME code SEC. VIII DIV.1 ED.2017		
	Joint categort	A	В	
Butt weld	Joint efficienc	1	1	
Dutt weld	Welding process	SMAW		
	Weld joint Groove	Double-V- groove		
P.W.H.T		YES		
Shell and head material		SA- 516 Gr.70N		
Saddle material		SA-285 Gr.C		

Table 2 Chemical composition of weld metal.

Chemical composition of weld metal					
	С	Mn	Si	S	P
AWS Standard	≤ 0.15	≤ 1.6	≤ 0.75	≤ 0.035	≤ 0.035
Typical	0.08	1.00	0.5	0.014	0.02

Table 3

I abic o					
Mechanical properties of weld metal. Mechanical properties of weld metal					
	Y.S (MPa)	T.S (MPa)	Elongation	Charpy V value	-
AWS Joint	≥ 400	≥ 490	≥ 22	$\geq 27j$	
Typical	480	570	30	127j	

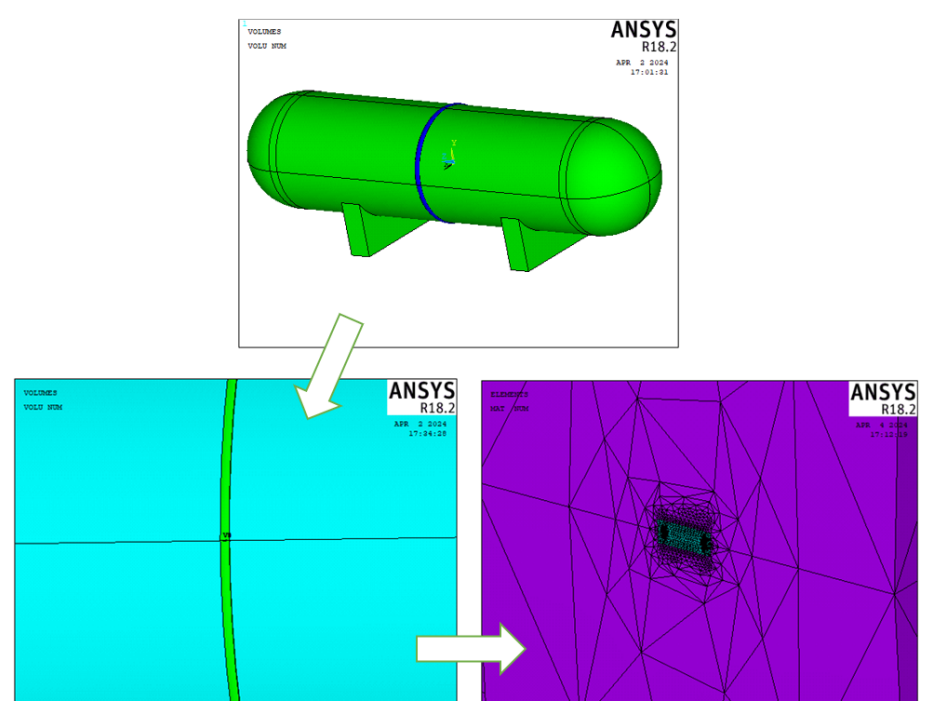


Fig. 9. General view of the crack model.

Quarter point elements are devised by Barsoum in 1976 [11] as an easy way to characterize the singularity of stress at the fracture tip. These are regular 8-node quadrilaterals or 6-node triangles with two mid-side points that have been moved to a corner node such that they split their side in a 1:3 ratio. The node where the mid-side nodes are shifted is where they are utilized,

namely at the crack tip. It is demonstrated that they provide an appropriate description of the $1/\sqrt{r}$ stress field singularity at the fracture tip.

Fig. 9 illustrates how various volumes are meshed with varying element sizes after the volume surrounding the fracture front has been meshed.

4. Convergence Study

An independent study of the mesh has been carried out for configuration, and the convergence study is conducted for the configuration as below:

The configuration was done based on a/c=1 and a/t=0.4. As shown in Fig. 10, The level of difference obtained with 41737 and 51023 elements was less than 1%. Therefore, the mesh with 41737 elements was used.

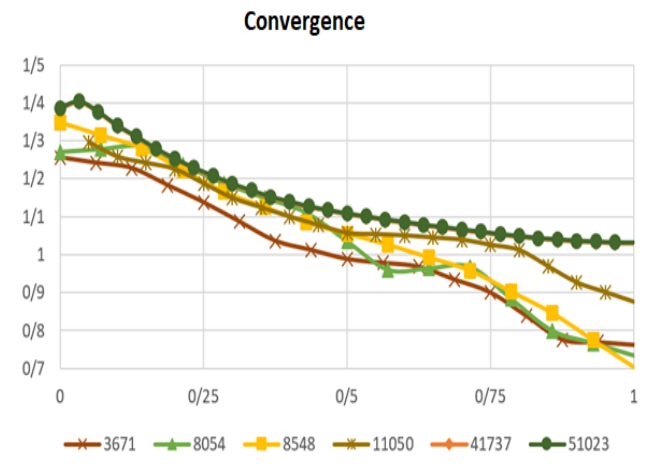


Fig. 10. Convergence study of normalized SIF (KI/Ko) for a semi-elliptical crack located in the elliptical pressure vessel. (a/c = 1 and a/t = 0.8).

Afterward, the results are compared with Raju and Newman [6], the current fracture model produces correct results and demonstrates rather good agreement, as seen in Fig. 11. The maximum variation is seen for a/t = 0.8 and a/c = 1 with a difference of 3 percent.

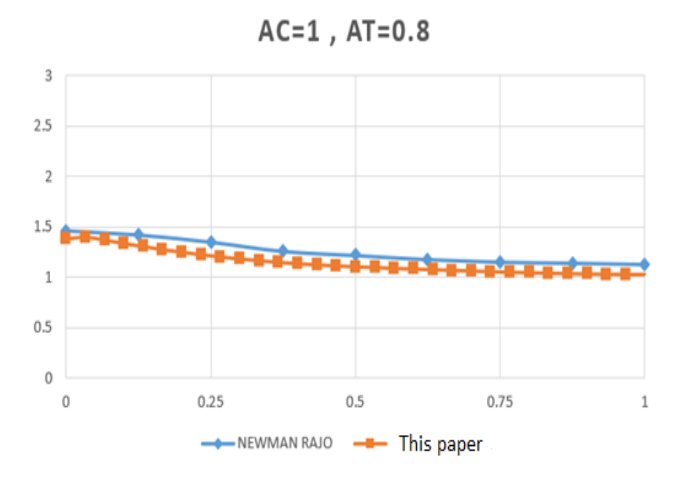


Fig. 11. Validation of fracture model with Newman and Raju for a semi-elliptical surface crack in a finite plate (a/t = 0.8 and a/c = 1).

Fig. 12 shows the final image of the crack opening as well as the maximum stress at the crack's tip; the red spots indicate maximum stress, while the blue points indicate minimum stress.

5. Numerical Results and Discussion

A wide range of parameters such as Ro/Ri, a/c stress intensity factor for semi-elliptical surface crack with ratios a/c = 0.4, 0.6, 0.8, 1 and 1.2 and a/t = 0.2, 0.4, 0.6, 0.8 and checking pressure and we have a comparison of the types of pressure inside the vessel.

The numerically calculated SIFs are normalized by k_0 , derived from the verification data. The SIF was calculated using Eq. (1).

$$K_0 = \frac{K}{S \sqrt{\pi \frac{a}{Q}}} \tag{1}$$

Where S is applied stress and Q is the shape factor. The X-axis $(\frac{2\Phi}{\pi})$ verification numbers were normalized.

For the x-axis numbers, the coordinates are divided by the crack tip to normalize it. To normalize the pressure, all k numbers are divided by the base pressure.

The effects and changes of K_I and K_0 for a semielliptical crack in an elliptical pressure vessel under mechanical loading were investigated. Due to symmetry, results for loading conditions (mechanical loading under compression only) are plotted for only one-half of the model. Fig. 13 illustrates the highest stress level at the crack front. Half of the crack surface is cracked after solving the element close to the crack front.

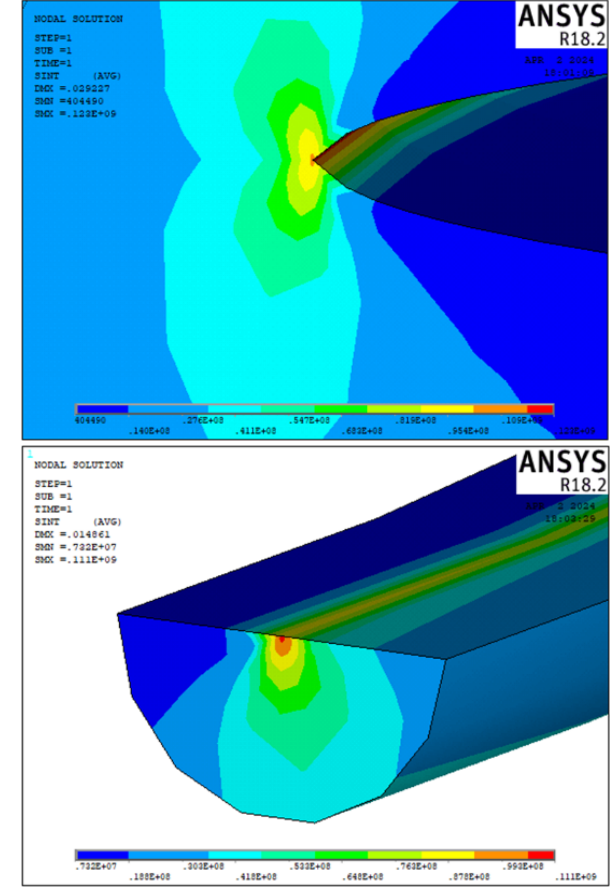


Fig. 12. Nodal solution of stress intensity factor at crack tip.

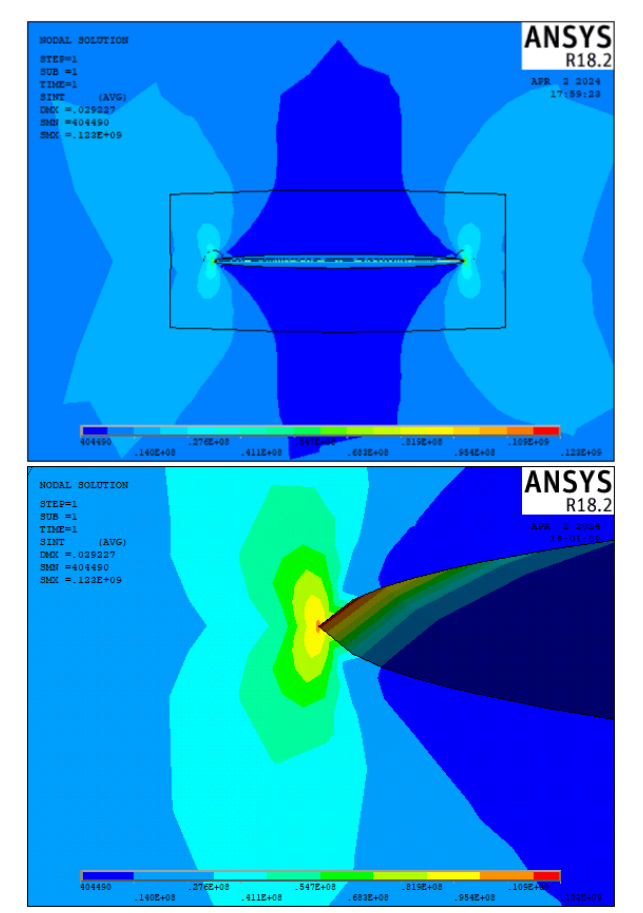


Fig. 13. Finite element model of an elliptical pressure tank containing a weld seam crack: a) The opening of the crack opening and the heart-shaped part in front of the crack. b) The crack opens due to the application of internal pressure, and the maximum intensity of stress is at the tip of the crack.

According to Fig. 13, it can be concluded that generally, deeper cracks have more KI/Ko. In another view, the lowest values of the normalized stress intensity coefficient are found near ~ 0.1 , and it is evident that the most significant and riskiest rate of fast crack growth occurs at point number 1, or the crack tip. However, to check this chart, a/c = 0.4 with blue line has the highest risk and prone to rapid crack growth, which should be taken into consideration. Moreover, a/c = 1 shows the lowest risk and slow crack growth rate.

5.1. Mode I Stress Intensity Factor (K_I)

Fig. 14 shows the stress distribution at the crack front of a semi-elliptical crack located at the weld seam of an elliptical tank subjected to internal pressure and tensile mechanical loading. With a/t=0.2 held constant and varying a/c ratios, the highest stress and crack growth rate are observed for a/c=0.4. Crack growth initiates at the crack tip and propagates longitudinally. The lowest crack growth rate corresponds to a/c=1.

Comparing the different values of a/t in Fig. 14, it can be concluded that by reducing the welding surface and reaching the tank shell at a low thickness in different studies from 0.2 to 0.8, it causes shallow cracks to become critical.

Of course, it should be noted that in Fig. 14, the curve related to a/c = 0.8 and a/t = 0.2 conditions does not coincide with the zero axis and it is far from the data related to the curve mentioned in Table 4.

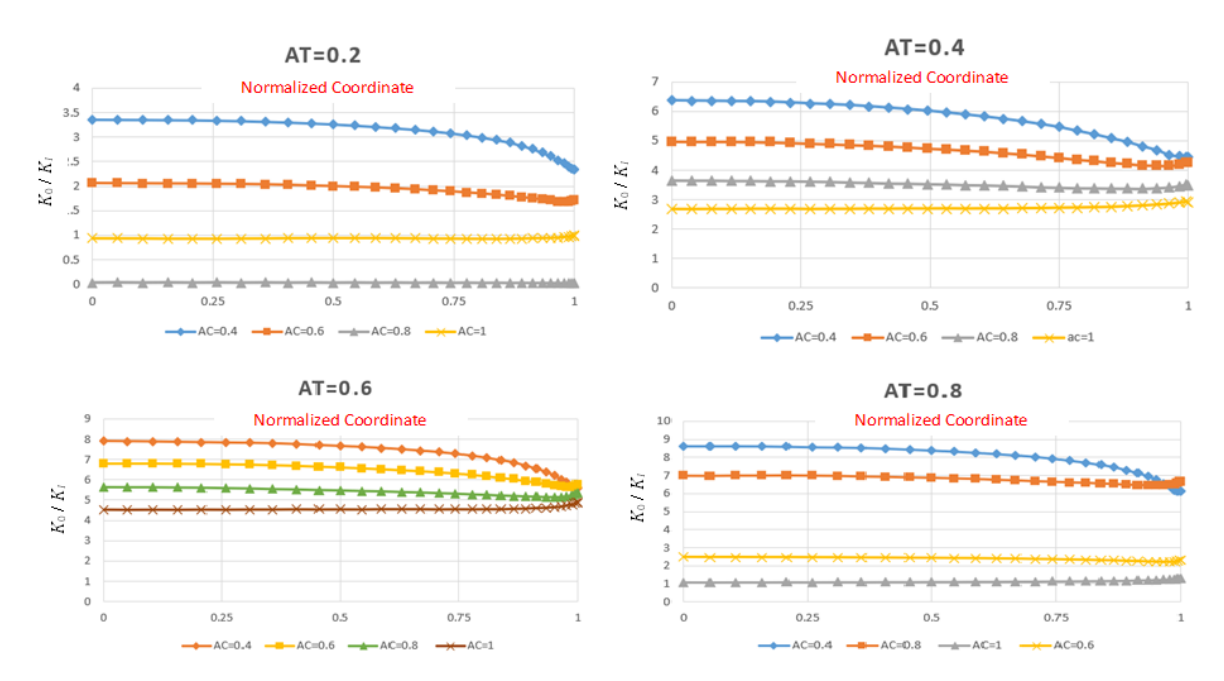


Fig. 14. Changes of K_I/K_0 in the length of the semi-elliptical crack front at the weld seam in the elliptical tank under internal pressure under mechanical loading as a function (at = 0.2, 0.4, 0.6, 0.8 and with different a/c).

Table 4 Values of $K0/K_1$ for a/c = 0.8 and a/t = 0.2.

K_{I}	KI-NORM AC=0.8	K_{I}	KI-NORM AC=0.9	K_{I}	KI-NORM AC=0.10
36301.9296	0.020486364	41921.6427	0.023657752	50832.1471	0.02868624
37387.0481	0.021098732	47808.9808	0.026980169	56205.8983	0.031718823
36679.8826	0.020699655	43888.1383	0.024767509	52094.91	0.029398859
38984.723	0.022000352	49971.7082	0.028200666	57319.3729	0.032347193
37229.9777	0.021010092	45962.2784	0.025938014	53199.8108	0.03002239
41086.4702	0.023186437	51947.8822	0.029315886	58224.0024	0.032857705
38441.0251	0.021693525	47821.7451	0.026987372	53997.3587	0.030472472
43390.2705	0.024486546	53628.5061	0.030264317	58826.4987	0.033197714
40076.5911	0.022616529	49484.3427	0.02792563	54532.3820	030774404
45682.3559	0.025780045	55028.7589	0.031054525	59204.02	0.033410762

From Fig. 15, it can be concluded that for a fixed a/c ratio, K_I/Ko increases with the crack depth ratio (a/t), indicating higher stress intensity and faster, more dangerous crack growth at the crack tip. Conversely, increasing the a/c ratio results in a decrease in K_I/Ko intensity.

In Fig. 15, it can be seen in the front extension of the semi-elliptical crack at the weld seam in the el-

liptical tank under internal pressure under tensile mechanical loading as a function (ac=0.4 constant and a/t varying) the highest stress and crack growth corresponding to a/t=0.8. Crack growth initiates at the crack tip. The highest stress is from that point and its growth is longitudinal, and the lowest crack growth corresponds to a/t=0.2.

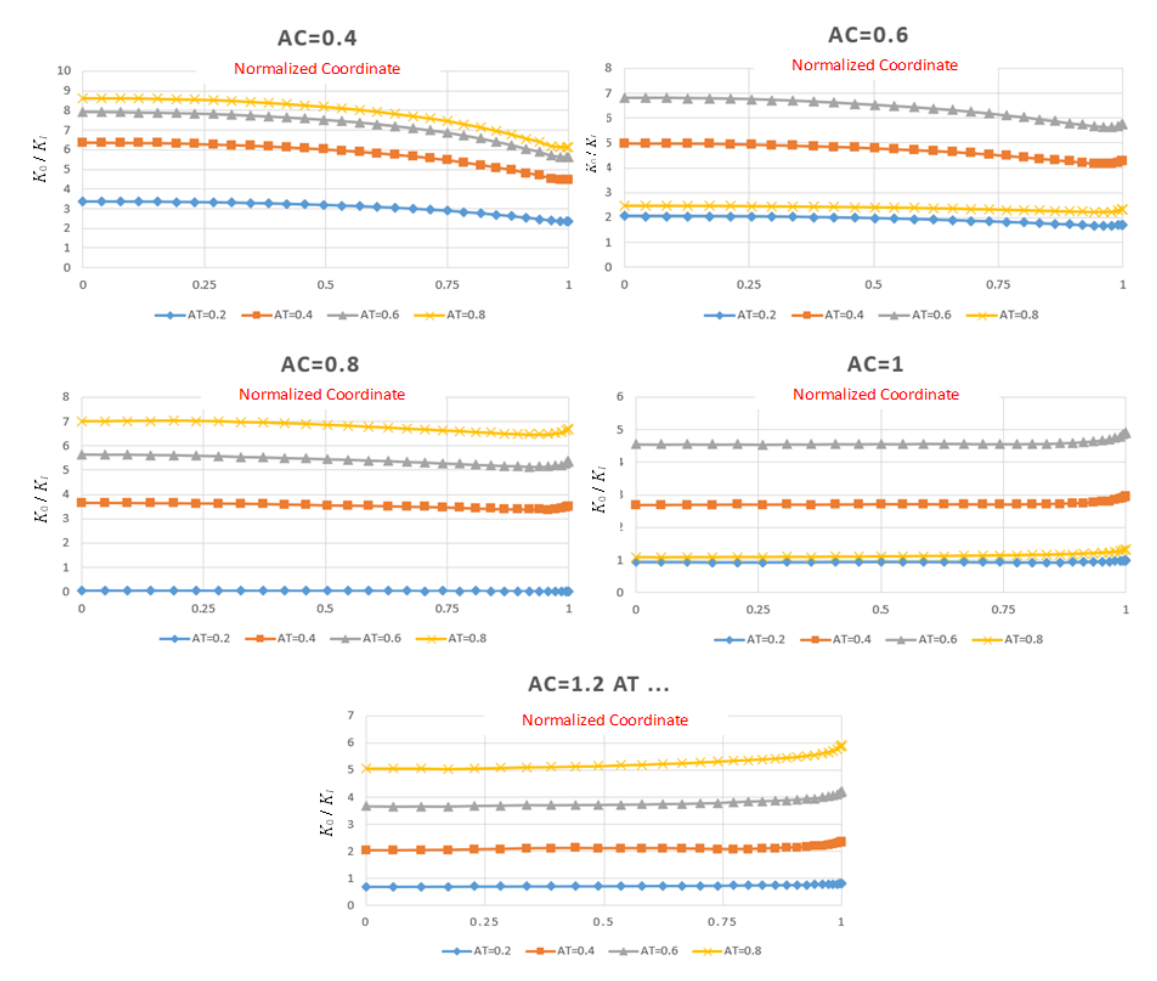


Fig. 15. Changes of K_i/K_0 in the length of the semi-elliptical crack front at the weld seam in the elliptical tank under internal pressure under mechanical loading as a function (ac = 0.4, 0.6, 0.8, 1, 1.2 constant and different a/t).

In Fig. 16, the comparison of the pressure inside the tank from a specific a/c and a/t from 5 to 20MPa is checked, indicating that the higher the pressure inside the tank, the faster the crack growth will be and it is more dangerous.

According to Fig. 16, it can be stated that along the front of the semi-elliptical crack at the weld seam in the elliptical pressure tank under internal pressure with a specified function (ac = 0.6 and at = 0.2), the maximum stress and crack growth are related to pressure. 20E6, which is critical and its growth from the crack tip, then the highest stress is from that point and its longitudinal growth, and the lowest crack growth is related to stress 5E6.

5.2. Mode II Stress Intensity Factor $(K_{\rm II})$

Based on Figs. 17-18, the distribution of the Mode II SIF at the crack front of a semi-elliptical crack located at the weld seam in an elliptical tank under internal pressure and shear loading shows values close to zero. Although various constant and varying a/c and a/t ratios were considered, significant Mode II SIF was not observed.

Based on Fig. 17, the distribution of the Mode II SIF at the crack front of a semi-elliptical crack located at the weld seam in an elliptical tank under internal pressure and shear loading shows values close to zero.

Although various constant and varying a/c and a/t ratios were considered, significant Mode II SIF was not observed.

5.3. Mode III Stress Intensity Factor (K_{III})

As observed in Figs. 19-20, the distribution of the Mode III SIF at the crack front of a semi-elliptical crack located at the weld seam in an elliptical tank under internal pressure and torsional loading is close to zero. Despite varying a/c and a/t ratios, no significant Mode III SIF was observed.

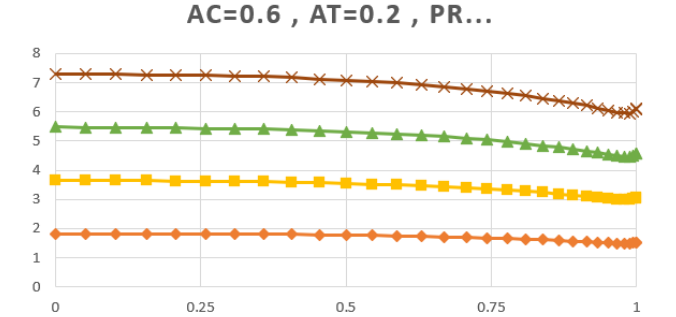


Fig. 16. K_o/K_I pressure changes along the semielliptical crack front at the weld seam in the elliptical pressure tank under internal pressure with a specified function (ac = 0.6 and at = 0.2).

→ PR=15E6 → PR=20E6

PR=10E6

-PR=5E6



Fig. 17. Distribution of the stress intensity coefficient in Mode II along the front of the semi-elliptical crack (a/t = 0.2, 0.4, 0.6, 0.8).

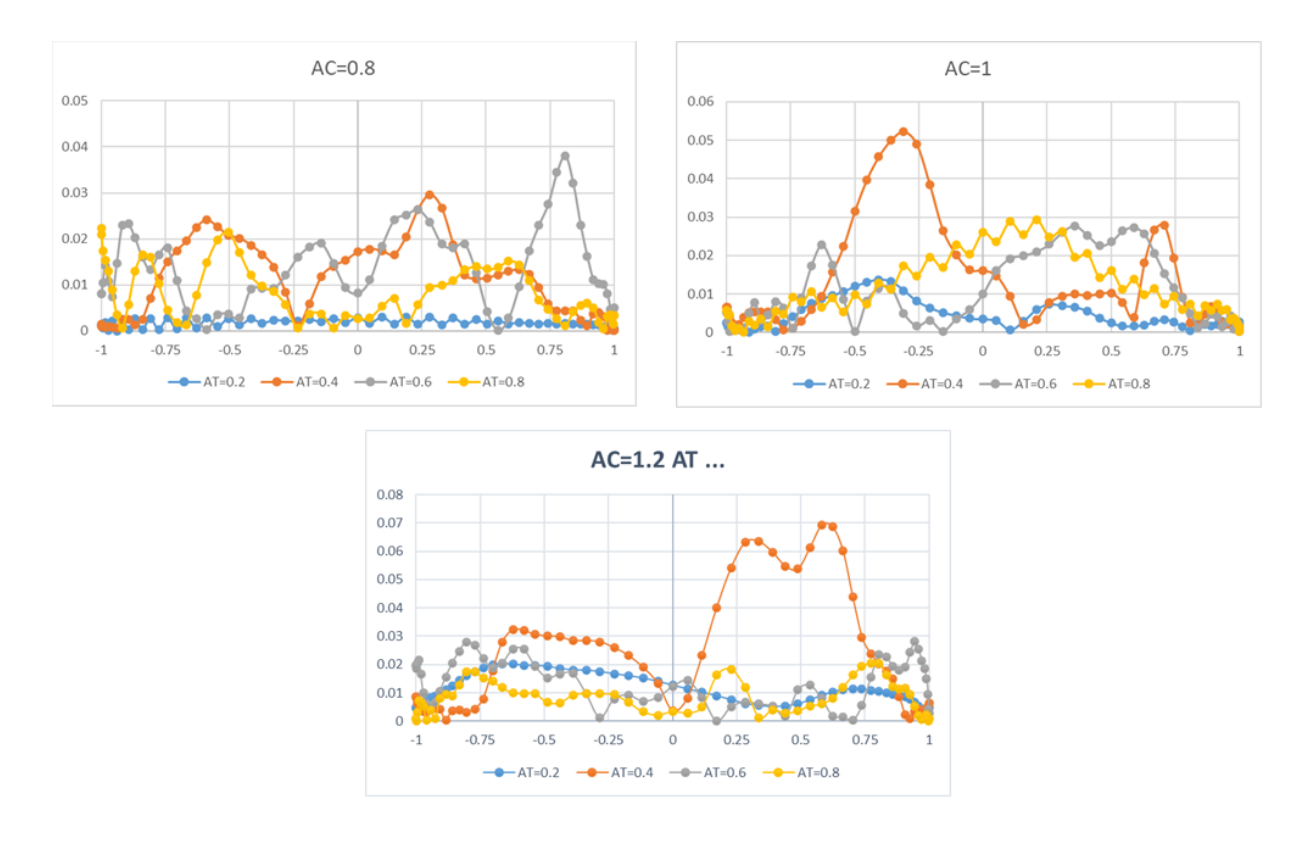


Fig. 18. Distribution of the stress intensity coefficient in mode II along the front of the semi-elliptical crack (a/c = 0.8, 1, 1.2, Different a/t values).



Fig. 19. Distribution of the stress intensity coefficient in state III in the semi-elliptical crack front extension (constant a/t = 0.2, 0.4, 0.6, 0.8, and different a/c).

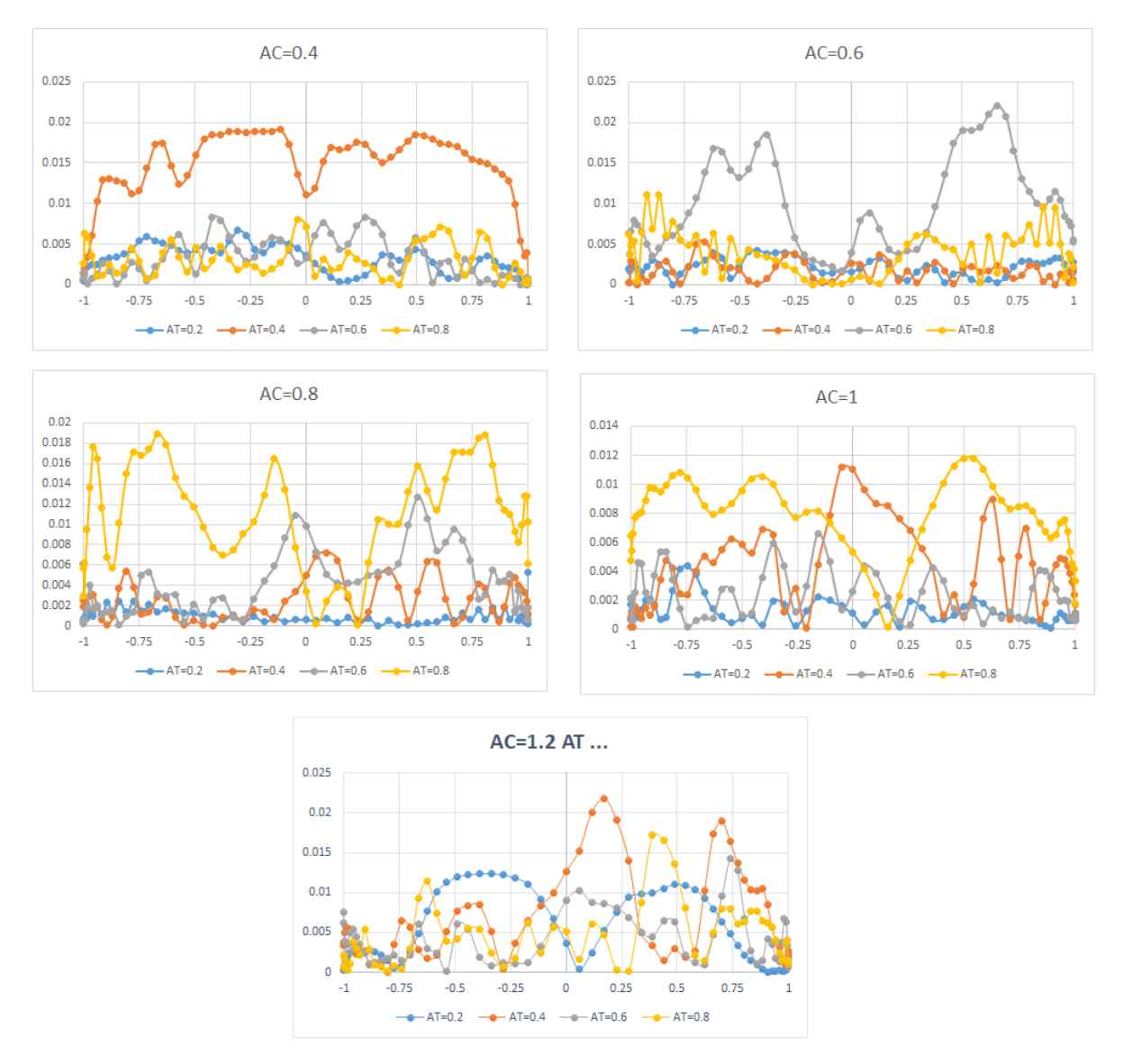


Fig. 20. Distribution of the stress intensity coefficient in state III in the semi-elliptical crack front extension (constant a/c = 0.4, 0.6, 0.8, 1, 1.2, and different a/t).

6. Conclusion

The Finite Element Technique (FEM) was used to conduct a three-dimensional study of an elliptical pressure vessel with a broken weld seam. The investigation focused on the impact of modifications to the stress field and geometric parameters on the semi-elliptical crack's SIF distribution.

In the weld joint area, a fracture with a distinct configuration is taken into consideration. The findings demonstrate that the stress distribution along a fissure may be greatly influenced by the vessel wall's thickness, the form and location of the crack, and the fact that shallower cracks pose a greater risk and need increased attention

In pressure states, the highest stress intensity factor is related to 20MPa pressure and the lowest stress

intensity factor is related to 5MPa pressure. As a result, values of internal pressure affect the levels of SIFs around the crack front, potentially leading to changes in the crack face. The residual stress is an interesting parameter that can be considered in further studies.

References

- Naser, Mohammed Qazam, and A. V. S. S. K. S. Gupta. "Structural and thermal analysis of pressure vessel by using ansys." International Journal of Scientific Engineering and Technology Research 2.8 (2013) 740-744.
- [2] V. V. W. S. S. M. D. D. P. H. S. B. P. P. Gavade, "DESIGN AND ANALYSIS OF PRESSURE VESSEL USING ANSYS," JOURNAL OF

- MECHANICAL ENGINEERING AND TECHNOLOGY (JMET), vol. 3, pp. 1-13, 2015.
- [3] K. G. Girase, N. K. Patil, D. Shinde, and K. Kalita, "Stress intensity factors for multiple cracks in thick-walled cylinder," International Journal of Scientific World, vol. 3, no. 2, pp. 207-215, 06/19 2015.
- [4] D. J. Wulpi, Understanding How Components Fail. 2013.
- [5] R. J. Sanford, Principles of Fracture Mechanics. Prentice Hall, 2003.
- [6] I. Raju and J. Newman, "Stress Intensity Factors for Internal Surface Cracks in Cylindrical Pressure Vessels," Journal of Pressure Vessel Technologytransactions of The Asme - J PRESSURE VES-SEL TECHNOL, vol. 102, no. 4, pp. 342-346, 11/01 1980.
- [7] X. Lin and R. Smith, "Fatigue Growth Prediction of Internal Surface Cracks in Pressure Vessels," Journal of Pressure Vessel Technology-transactions of The Asme J PRESSURE VESSEL TECHNOL, vol. 120, no. 1, pp. 17-23, 02/01 1998.
- [8] X. B. Lin and R. A. Smith, "Shape growth simulation of surface cracks in tension fatigued round bars," International Journal of Fatigue, vol. 19, no. 6, pp. 461-469, 1997/08/01/1997.
- [9] S. T. Lie, H. S. Zhao, and S. P. Vipin, "New weld toe magnification factors for semi-elliptical cracks in plate-to-plate butt-welded joints," Fatigue & Fracture of Engineering Materials & Structures, vol. 40, no. 2, pp. 207-220, 2016.

- [10] T. Meshii and K. Watanabe, "Stress intensity factor for a circumferential crack in a finite-length thin to thick-walled cylinder under an arbitrary biquadratic stress distribution on the crack surfaces," Engineering Fracture Mechanics, vol. 68, no. 8, pp. 975-986, 2001/05/01/2001.
- [11] G. G. Cabbon Eachan, Iba Jabali, Label Naa-garjun, Adalbert Baadal, "Semi-Elliptical Surface Crack in Pressure Vessel: Analysis and Assessment," World Information Technology and Engineering Journal, vol. 11, 2023.
- [12] N. Habibi and H. Bahrampour, "Estimation of the SIF in FGM spherical pressure vessel," Australian Journal of Mechanical Engineering, vol. 20, no. 4, pp. 911-926, 2020, doi: 10.1080/14484846.2020.1762965.
- [13] W. W. Sadavir Udichi, Yachika Zacarias, Cabbon Eachan, Adalbert Baadal, "Researching the Influence of Semi-Elliptical Crack on the Failure of Pressure Vessels Operating Finite Element Analysis," European Journal of Scientific and Applied Sciences, vol. 10, 2023.
- [14] I. J. Gabai Gabor, Label Naagarjun, Obaid Paal, Adalbert Baadal, "Investigating the Effect of Semi-Elliptical Crack on the Failure of Pressure Vessels Using Finite Element Analysis," Asian Journal of Basic and Applied Sciences, vol. 10, 2023.
- [15] N. Javid and M. Amini, "Evaluating the effect of supply chain management practice on implementation of halal agroindustry and competitive advantage for small and medium enterprises," International Journal of Computer Science and Information Technology, vol. 15, pp. 8997-9008, 01/01 2023.